Progress In Electromagnetics Research, PIER 65, 125–136, 2006

POLARIZED OPTICAL ORTHOGONAL CODE FOR OPTICAL CODE DIVISION MULTIPLE ACCESS SYSTEMS

N. Tarhuni

Communications Engineering Lab
Helsinki University of Technology
Otakaari 5A 02150 Espoo, Finland

M. Elmusrati

Control Engineering Lab
Helsinki University of Technology
Otaniementie 17 02150 Espoo, Finland

T. Korhonen

Communications Engineering Lab
Helsinki University of Technology
Otakaari 5A 02150 Espoo, Finland

Abstract—In this paper a Polarized Optical Orthogonal Code (Polarized-OOC) is proposed by exploiting the polarization property of the fiber and the chip's polarization state. The polarized-OOC code is generated using the concept of Mark Position Difference (MPD) set. Polarized-OOC code cardinality is shown to be two times that of the conventional OOC which reflects an increase in the number of supported users. Furthermore, since the correlation properties of the constructed code are the same as that of conventional OOC, error rate performance is evaluated in the same way as in conventional OOC. Also, a simple procedure for fiber-induced polarization rotation compensation is introduced. We then use simulations to show that relative polarization axis misalignment between the desired user and interfering users leads to violation of the correlation properties of the proposed code.

1. INTRODUCTION

A multiple access scheme such as optical CDMA (OCDMA) is required to make full use of the available bandwidth in optical fibers. OCDMA features accommodation of a number of channels on a single carrier frequency, enabling soft capacity and enhanced security [1, 2]. A channel in a CDMA system occupies the same frequency-time space as all the other CDMA channels. Each CDMA channel is distinguished from other CDMA channels by a unique CDMA spreading code. Different codes have been developed specifically for use in optical CDMA (OCDMA) systems. A class of codes proposed in [3] called Optical Orthogonal Codes (OOC). The OOC is designed to satisfy certain correlation properties, namely, a high autocorrelation peak proportional to code weight, and a non-zero shift autocorrelation and crosscorrelation values bounded by one. Each chip in the OOC intensity modulates the laser source in the transmitter. It was assumed that the optical chips have the same polarization. The OCDMA scheme has the following advantages [1, 2]:

- Passive optical devices can be used to address OCDMA channels (unlike in WDM).
- OCDMA can increase data throughput in point-to-point links, when combined with, or in place of WDM.
- OCDMA supplies user-specific connections without electronic overhead required for the same function in TDM.
- OCDMA systems enable contention-free multiuser networks operating on a single optical carrier frequency.

To implement OCDMA system, it is necessary to have:

- Suitable optical-code designs.
- Robust and cost-effective generation of coded bits.
- Detecting bits in a code specific manner.
- Suppression of cross talk from other code channels (multi-user interference)

Polarization Shift Keying (PolSK) was considered during recent years as a digital modulation candidate for the optical fiber communications [4, 5]. It is applicability is a result of the property that an orthogonal state of polarization (SOP) pair from a monochromatic light source at the input of the Single Mode Fiber (SMF) leads to orthogonal SOP pair at the fiber output, although the input SOP is not maintained in general. PolSK has many advantages including high insensitivity to laser phase noise, increased resistance to self-phase modulation and cross-phase modulation. Previous experimental

work showed that the depolarization phenomena along the fiber and polarization dependent losses are negligible even after relatively long fiber spans [6–8]. Measurements on buried SMF fibers (18, 23.7 and 13.9 km links) reported in [9] reveal that polarization fluctuations are quite slow and can vary typically between 2^o-10^o per day.

In this paper the polarization of the individual chips is used in order to double the OOC code cardinality aiming to increase network capacity. The paper is organized as follows: In Section 2 the code construction is presented. Section 3 shows the Polarized-OOC system, polarization rotation compensation and performance analysis. Finally numerical analysis and conclusions are drawn at the end of the paper.

2. POLARIZED-OOC CODE CONSTRUCTION

The OOC codeset $\mathbf{C}$ is characterized by $(N, W, \lambda_a, \lambda_c)$ where N, W, λ_a and λ_c are the code length, code weight (number of ones in the code), maximum non-zero shift autocorrelation and maximum cross-correlation, respectively. The following periodic correlation conditions are satisfied by conventional OOCs, and by Polarized-OOC [3],

$$R_{xx}(m) = \sum_{n=0}^{N-1} x_n x_{n+m} \leqslant \lambda_a \tag{1}$$

for any $x \in \mathbf{C}$ and any integer $[m]_{\mathrm{mod}(N)} \neq 0$, where $[m]_{\mathrm{mod}(N)}$ denotes m modulo N, and,

$$R_{xy}(m) = \sum_{n=0}^{N-1} x_n y_{n+m} \leqslant \lambda_c \tag{2}$$

for any $(x \neq y) \in \mathbf{C}$ and any integer m. We consider only the case that will lead to the lowest possible Multiple Access Interference (MAI) in which $(\lambda_a = \lambda_c = 1)$ and the code is denoted by the pair (N, W).

For and two OOC codes c_i and c_j the Mark Position Difference (MPD) sets are denoted by d_i and d_j. The MPD elements are integers representing the distance between the different chips composing the code [10]. To satisfy the OOC correlation properties, it is required that there should be no repeated elements in the code MPD and no common elements between the MPDs of any two codes. Specifically, the conditions in (1) and (2) are satisfied if there are no repeated elements in d_i or d_j, and no shared elements between d_i and d_j.

For conventional OOC the number of supported users was found

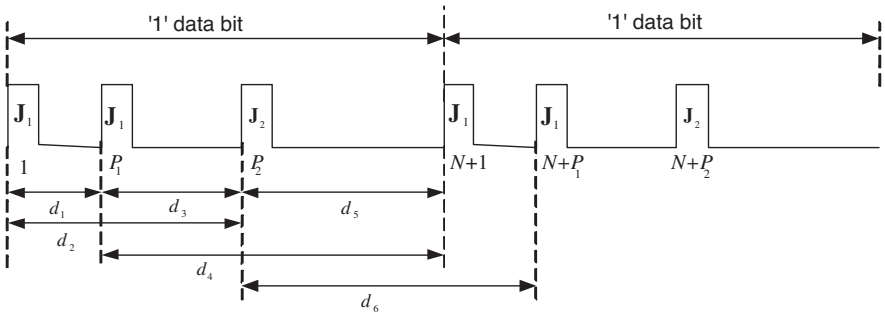

Figure 1. Mark positions and differences for a (N,3) polarized-OOC.

to be upper bounded by [3],

$$K_1 \leqslant \left\lfloor \frac{N-1}{W(W-1)} \right\rfloor \tag{3}$$

where $\lfloor x \rfloor$ is the integer part of x.

In Polarized-OOC the SOP of the pulses are rotated arbitrarily to two orthogonal SOPs. In Jones space the SOP of the optical beam is represented by $\mathbf{J} = [E_x, E_y]^T$ where E_x and E_y are the complex amplitudes of the x- and y-components of a field traveling in the z direction. The corresponding Stoke vector is denoted by $\hat{\mathbf{S}} = [S_1, S_2, S_3]^T$, where $S_1 = |E_x|^2 - |E_y|^2$, $S_2 = 2|E_x||E_y|\cos(\phi)$, and $S_3 = 2|E_x||E_y|\sin(\phi)$; with $\phi = \angle E_y - \angle E_x$. Two polarization states represented by $\mathbf{J}_1$ and $\mathbf{J}_2$ are orthogonal if the inner product is zero, i.e., $\mathbf{J}_1^H \mathbf{J}_2 = E_{1x}^* E_{2x} + E_{1y}^* E_{2y} = 0$, where H is the Hermitian.

The MPD elements can be deduced by considering two consecutive encoded data bits of '1' as shown in Fig. 1, then Polarized-OOC code is generated as follows. The individual chips are marked with the corresponding Jones vector representing one of a two possible orthogonal SOPs. The position of the W individual chips of the k-th user code is denoted by $c_k = [1, P_1, P_2, ..., P_W]$, the sign of P_i indicates the SOP. For a positive signed P_i the SOP is $\mathbf{J}_1$ and for a negative signed P_i the SOP is $\mathbf{J}_2$. Then the MPD is given by,

$$d_k = \{\mathrm{sgn}(P_i) \times \mathrm{sgn}(P_j) \left[N - [N + |P_i| - |P_j|]_{mod(N)} \right]\} \tag{4}$$

for $i \neq j$ and $i, j = 1, 2, ..., W$; where sgn() is the sign operator. Now, the possible differences in (4) can be only in the set of integer numbers as,
$\mathbf{D}_{Polarized-OOC} = \{-(N-1), -(N-2), ..., -2, -1, 1, 2, ..., (N-1)\}$.

For conventional OOCs the possible difference is given by $\mathbf{D}_{OOC} = \{1, 2, ..., (N-1)\}$ [10]. Comparing the two sets it is clear that $|\mathbf{D}_{Polarized-OOC}| = 2|\mathbf{D}_{OOC}|$, which leads to doubling of the number of codes, where $|\mathbf{D}|$ denotes the number of elements in $\mathbf{D}$. Assuming that we have K_2 codes in the Polarized-OOC codeset. Since for each code the MPD length is $W(W-1)$ and the total possible differences are $2(N-1)$ then $K_2W(W-1) \leqslant 2(N-1)$. Therefore, the number of codes in the Polarized-OOC is upper bounded by,

$$K_2 \leqslant \left\lfloor \frac{2(N-1)}{W(W-1)} \right\rfloor \tag{5}$$

Codesets with $(N, W) = (300, 3)$, $(500, 4)$, and $(700, 5)$ with cardinalities (using (5)) of 99, 83, and 69 respectively are generated using the algorithm applied in [10] and tabulated in Table 1. Due to space limitations only a subset of the codes are shown. Considering the first and second codes under the (300,3) Polarized-OOC in Table 1, the corresponding MPDs following (4) are $d_1 = \{-143, -251, 108, -157, -49, 192\}$ and $d_2 = \{237, -250, -13, 63, -50, -287\}$. Since there are no repeated elements in d_1 or d_2, and no shared elements between d_1 and d_2, therefore, the two codes are part of the Polarized-OOC code set. A simple and specific example to show code cardinality doubling when Polarized-OOC is used is the following. Consider a 2-code (13,3) conventional OOC code set $\mathbf{C}_{OOC} = \{[1, 6, 12], [1, 4, 5]\}$ and compare to a 4-code Polarized-OOC with the same length and weight $\mathbf{C}_{Polarized-OOC} = \{[1, 2, 6], [1, 7, -9], [1, -11, 12], [1, -5, 11]\}$. It is also straightforward to extend the Polarized-OOC for multiclass traffic as in [10] by defining the possible MPD sets for the different classes according to the code length of each class and then start the code generation procedure with the shortest-length class.

3. POLARIZED-OOC SYSTEM

Figure 2 shows a complete OCDMA system based on Polarized-OOC. Following the basic OOC system proposed in [3] in which optical pulses are modulated by the data bits using an ON/OFF modulator and then encoded optically to produce the OCDMA signal. We assume rectangular optical pulses for simplicity but dispersion managed Gaussian and super-Gaussian solitons with enhanced properties can also be used [11]. In our case the encoding operation of the code chips includes the rotation of the SOP of the optical beam. The encoder can be implemented with a network of $(W-1)$ optical delay lines and $(W-1)$ polarization rotators chosen according to a Polarized-OOC

Table 1. Polarized-OOC code sets.

(300,3)	(500,4)	(700,5)
$[1, -144, -252]$	$[1, -210, 214, -430]$	$[1, -15, -153, -192, 275]$
$[1, 238, -251]$	$[1, 253, -274, -311]$	$[1, 192, 208, 252, -536]$
$[1, 81, 90]$	$[1, 144, -238, -401]$	$[1, -151, 198, 468, 639]$
$[1, -203, 255]$	$[1, -356, -447, 478]$	$[1, -59, 64, 389, 437]$
$[1, -190, 245]$	$[1, 60, 314, -461]$	$[1, 246, -247, 263, -347]$
$[1, -80, 214]$	$[1, -125, -272, 441]$	$[1, -72, -366, -623, 666]$
$[1, -10, -175]$	$[1, -209, 254, 483]$	$[1, -477, 537, -566, 677]$
$[1, 56, 106]$	$[1, -145, -263, -495]$	$[1, -90, 146, -458, -540]$
$[1, -255, 284]$	$[1, -62, -218, 450]$	$[1, -283, 386, 396, 462]$
$[1, 40, 149]$	$[1, -126, -160, 294]$	$[1, 145, 225, 323, -476]$

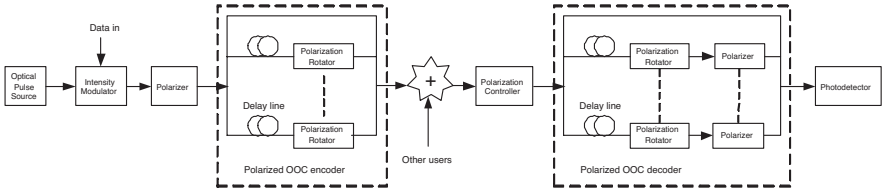

Figure 2. OCDMA setup based on Polarized-OOC encoding and decoding.

code generated as in Section 2. A beam splitter and combiner is also required which give rise to optical power loss. For flexible addressing, an encoder with tunable optical delays and tunable polarization rotators can be used. Hence, the SOP encoded signal travels a distance of L [km] through an SMF. Consequently, the SOP-encoded signal undergoes several impairments such as, attenuation, polarization rotation, fiber nonlinearity, several dispersion mechanisms. SOP rotation is compensated by applying the received SOP encoded signal to the polarization SOP control block whose function is to insure that the received signal and the optical components at the receiver have the same SOP reference axis. In order to compensate for SOP fiber induced rotation we propose the following simple technique. We assume that a reference SOP $\hat{\mathbf{S}}_t$ is launched at the fiber input and the received SOP at the fiber output is $\hat{\mathbf{S}}_r$. A matrix $\hat{\mathbf{R}}$ that can rotate $\hat{\mathbf{S}}_r$ around

$\hat{\mathbf{S}}_{av} = [S_{av1}, S_{av1}, S_{av1}]^T = (\hat{\mathbf{S}}_t + \hat{\mathbf{S}}_r)/2$ by an angle β is given by [12],

$$\hat{\mathbf{R}} = \cos(\beta)\mathbf{I} + (1 - \cos(\beta))[\hat{\mathbf{S}}_{av}\hat{\mathbf{S}}_{av}] + \sin(\beta)\hat{\mathbf{S}}_{av} \times \tag{6}$$

where,

$$[\hat{\mathbf{S}}_{av}\hat{\mathbf{S}}_{av}] = \left(\begin{array}{ccc} S_{av1}\hat{\mathbf{S}}_{av}, & S_{av2}\hat{\mathbf{S}}_{av}, & S_{av3}\hat{\mathbf{S}}_{av} \end{array} \right)$$

and

$$[\hat{\mathbf{S}}_{av}\times] = \left(\begin{array}{ccc} 0 & -S_{av3} & S_{av2} \\ S_{av3} & 0 & -S_{av1} \\ -S_{av2} & S_{av1} & 0 \end{array} \right)$$

Then, to compensate for SOP rotation, the received SOP $\hat{\mathbf{S}}_r$ is rotated around $\hat{\mathbf{S}}_{av}$ by an angle of $\beta = \pi$. This is demonstrated for arbitrarily selected $\hat{\mathbf{S}}_t$ and $\hat{\mathbf{S}}_r$ that is rotated around $\hat{\mathbf{S}}_{av}$ for $\beta = 0$ to π in steps of 10^o as shown in Fig. 3.

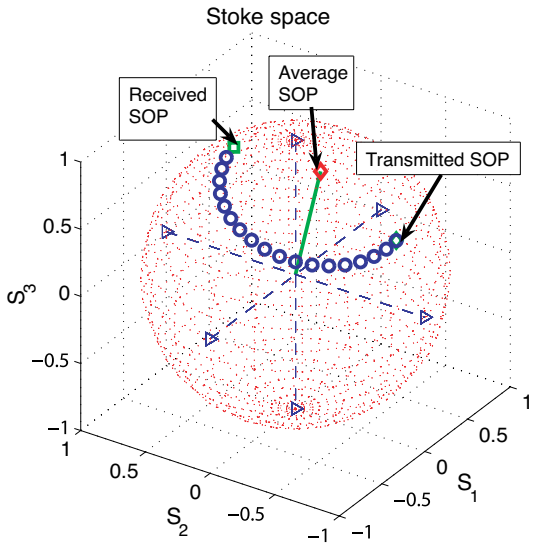

Figure 3. Rotation of arbitrarily received SOP to the reference SOP around the average SOP.

The polarized-OOC decoder then performs the correlation operation by passing the signal through a matched network of $(W-1)$ delay lines, $(W-1)$ polarization rotators, and $(W-1)$ polarizers. At the output of the delay lines the desired user code chips are aligned.

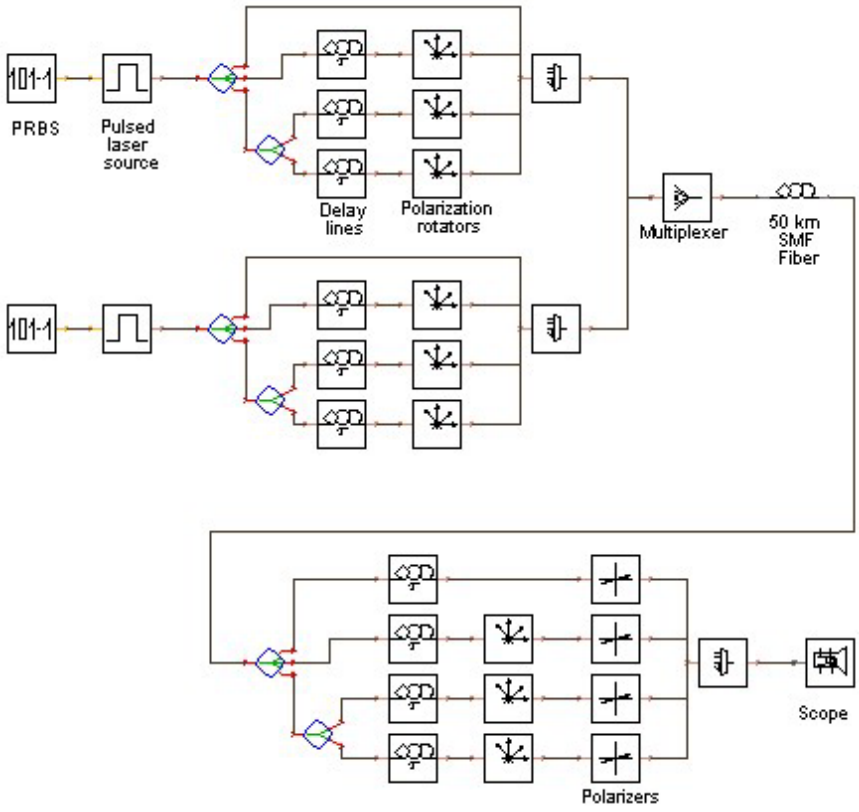

Figure 4. VPI simulation setup for two-user Polarized-OOC.

Then their SOP is rotated by polarization rotators matched to those applied at the encoder. Next the polarizers prevent other codes with matched delay but different SOPs from passing through, therefore, MAI is reduced to a binomially distributed random variable as in conventional OOCs. Finally, the output of the decoder will be a signal with a central high optical peak which is proportional to the code weight.

Since the proposed Polarized-OOC code satisfies (1) and (2) for $\lambda_a = \lambda_c = 1$, then the BER performance analysis of the Polarized-OOC will be the same as of conventional OOC. Therefore, at the sampling instant each interfering signal will introduce a single interfering pulse

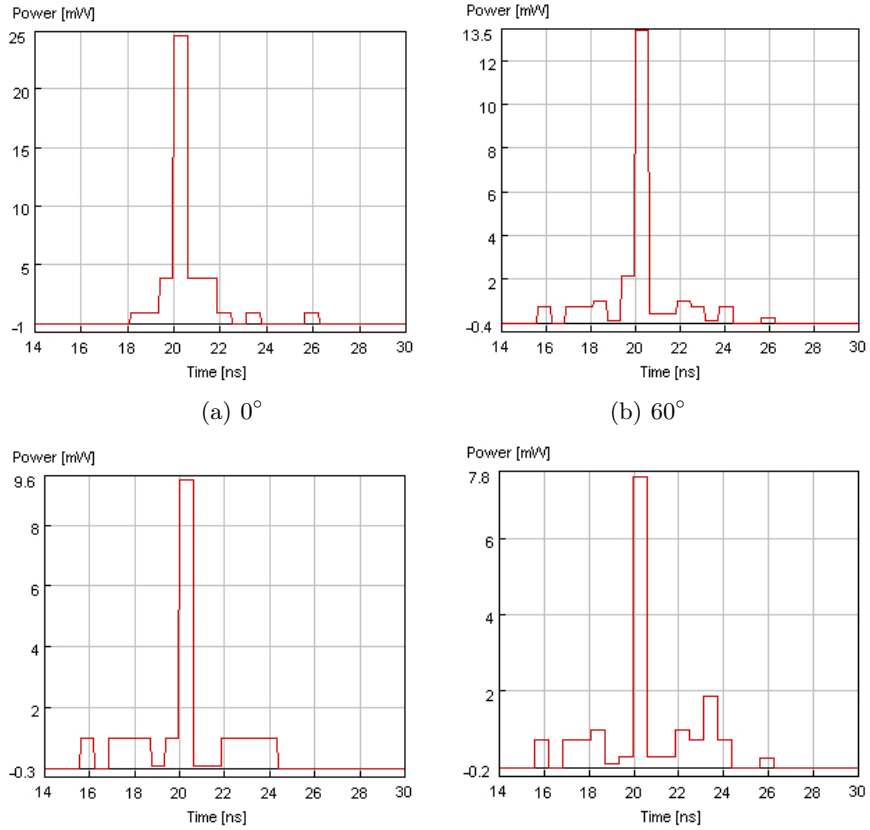

(a) 0° (b) 60°

(c) 90° (d) 120°

Figure 5. Correlator output in a two-user Polarized-OOC VPI simulation setup for different polarization axis misalignment of the interfering user and fibers excluded.

which will lead to the known bit error probability [3],

$$P(E) = \sum_{i=\mu}^{K_2-1} \binom{K_2-1}{i} \left(\frac{W^2}{2N}\right)^i \left(1-\frac{W^2}{2N}\right)^{K_2-1-i} \tag{7}$$

where μ is the threshold. In (7) the received optical powers from all users are assumed to be equal. When received optical powers from the different users are not the same then power control techniques [13] can be applied to mitigate the near-far effect due to the MAI.

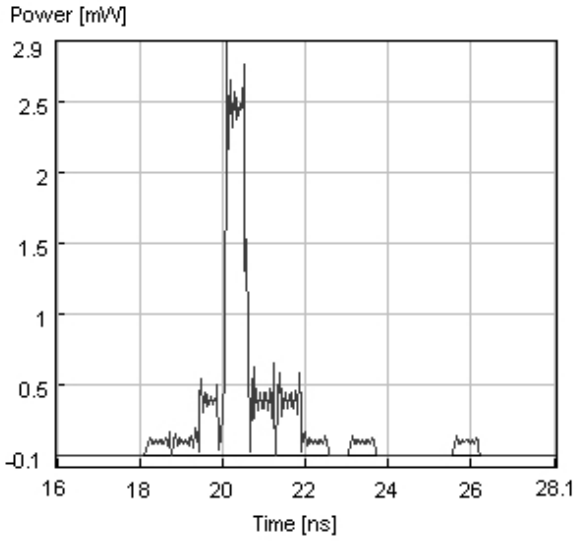

Figure 6. Correlator output with fiber included.

4. NUMERICAL RESULTS

The VPI systems optical simulator is used to simulate a two-user Polarized-OOC optical system shown in Fig. 4. Each user applies a $(16, 4)$ Polarized-OOC code, the total signal travels through an SMF with the following characteristics: length of 50 km, attenuation coefficient of 0.2 (fast and slow axis are equal), dispersion of $16e^{-6}$ [s/m^2], and polarization mode dispersion $3.16e^{-14}$ [s/m$^{1/2}$] (which is equivalent to a mean DGD of 10 ps over a distance of 100 km). The data rate is 100 Mbit/sec which means a chip rate of 1.6 Gchip/sec. In Fig. 5 a sample function of the output of the first user is shown for different polarization axis misalignment of the interfering user. Even though the level of the detected signal is generally reduced for a misaligned receiver polarization axis, clear peaks in the correlator output can be detected and transmitted data can be easily recovered. Also, since the interfering user polarization axis is rotated relative to the desired user, consequently the polarization relations assumed when the Polarized-OOC is designed are violated. This leads to violation of the correlation constraints and we can see this in the multilevel result shown in Fig. 5. The result depicted in Fig. 5 is obtained with the fiber excluded or a back-to-back simulation. Hence the peaks of the pulses are rectangularly shaped similar to the applied signal at the

transmitter. When the fiber is included, fluctuations and overshot of the output signal peaks results due to fiber-induced SOP rotations as shown in Fig. 6. Therefore, PMD compensation is expected to reduce these effects.

5. CONCLUSIONS

In this paper we proposed the use of polarized optical chips. Using this concept we were able to design Polarized-OOC with doubled number of users as compared to conventional OOCs. We demonstrate how the Polarized-OOC signal can be generated using a network of optical delay lines and polarization rotators. On the decoder side extra polarizers are needed to prevent interfering user chips with the same delay but different SOP from building MAI. A simple algorithm for polarization rotation compensation is also presented. Code construction based on mark position differences was used to construct several codesets. Performance of the Polarized-OOC in terms of error rates is given in a simple and straightforward way.

REFERENCES

1. Kitayama, K., H. Sotobayashi, and N. Wada, "Optical Code Division Multiplexing (OCDM) and its applications to photonic networks," *IEICE Trans. Fundamentals*, Vol. E82-A, No. 12, Dec. 1999.
2. Mossberg, T. W. and M. G. Raymer, "Optical Code-Division Multiplexing," *Optics and Photonics News*, March 2001.
3. Salehi, J., "Code division multiple access techniques in optical fiber networks—Part I: Fundamental concepts," *IEEE Trans. Comm.,* Vol. 37, 824, August 1989.
4. Calvani, R., et al., "Polarization shift keying: An coherent transmission technique with differential heterodyne detection," *Electron. Lett.*, Vol. 24, 642–643, May 1988.
5. Benedetto, S. and P. Poggiolini, "Theory of polarization shift keying," *IEEE Transactions on Communications,* Vol. 40, Issue 4, 708–721, April 1992 .
6. Poole, C. D., et al., "Phenomenological approach to polarization in long single-mode fibers," *Electron. Lett.*, Vol. 22, No. 19, 1029–1030, Sept. 11, 1986.
7. Cimini, L. G., et al., "Preservation of polarization orthogonality through a linear optical system," *Electron. Lett.*, Vol. 23, No. 23, 1365–1366, Dec. 3, 1987.

8. Poole, C. D., et al., "Polarization dispersion and principal states in a 147-km undersea lightwave cable," *J. Lightwave Technology*, Vol. 6, 1185–1190, July 1988.
9. Nichlson, G. and D. Tempe, "Polarization fluctuation measurements on installed single-mode fibre," *J. Lightwave Technology*, Vol. 7, Issue 8, 1197–1200, 1989.
10. Tarhuni, N., T. Korhonen, E. Mutafungwa, and M. Elmusrati, "Multi-class optical orthogonal codes for multi-service optical CDMA networks," *Journal of Lightwave Tech.*, Vol. 24, No. 2, February 2006.
11. Biswas, A. and S. Konar, "Theory of dispersion-managed optical solitons," *Progress In Electromagnetics Research*, PIER 50, 83–134, 2005.
12. Gordon, J. P. and H. Kogelnik, "PMD fundamentals: Polarization mode dispersion in optical fibers," *PNAS*, Vol. 97, No. 9, April 25, 2000.
13. Tarhuni, N., M. Elmusrati, and T. Korhonen, "Multi-class optical-CDMA network using optical power control," *Progress In Electromagnetics Research*, PIER 64, 279–292, 2006.